Proceedings of Engineering and Technology Innovation, vol. 10, 2018, pp. 29 - 33

Battery Management System for 24-V Battery-Powered Electric Wheelchair

Tzu-Hsiang Tseng*, Liang-Rui Chen, Yu-Jia Zhang, Bo-Rui Xu, Jin-An Li

Department of Electical Engineering, National Changhua University of Education, Changhua, Taiwan, ROC

Received 25 April 2018; received in revised form 30 May 2018; accepted 13 July 2018

Abstract

This paper describes a simplified battery-management system using a digital signal processor for a 24-V battery-powered electric wheelchair to modulate and protect the battery from operating outside its safe operating area, such as over-temperature, under-temperature, over-voltage, under-voltage, over-current discharge, or over-current charging. Using the buck-boost circuit topology, we achieved and demonstrated both battery balance and protection in a prototype 12-V/40-Ah series-connected two-battery module. Simulation results show that the proposed battery management system is feasible for a 24-V battery-powered electric wheelchair application.

Keywords: battery management system (BMS), digital signal processor, battery balance, battery protection

1. Introduction

With the rapid development of science and technology, traditional hand-propelled wheelchairs have gradually evolved into electrically powered wheelchairs that can be operated by individuals with mobility impairments [1-2]. Recently, a wide variety of electric wheelchairs have emerged, including solar hybrid wheelchairs [3] and four-wheel-drive wheelchairs [4].

As various forms of electric wheelchairs continue to develop, energy sources, cost-effectiveness, and safety is also becoming increasingly more important topics of discussion [5-7]. Electric wheelchairs malfunctions have been reportedly causing potential traffic concerns. Power system diagnosis showed the majority of the incidents and damages to the system were caused by imbalanced or unprotected batteries.

In this study, we developed a battery-management system (BMS) for electric wheelchairs. The electric motors of commercial electric wheelchairs are commonly powered by batteries. A single battery can only supply limited voltage and capacity and has a shorter battery life under a high-power state compared to multiple batteries. To operate in a high-voltage and high-power state, serially connected batteries are often used. However, balancing the capacity in serially connected batteries becomes a challenge as the batteries are often not identical, with capacity variance resulting from the manufacturing process, battery usage, such as repeated charging and discharging, or extended applications in a high-power state causing over-discharge. This results in an imbalanced capacity and voltage among serially connected batteries, which affects the overall lifespan and energy loss of the batteries.

Many research articles [8-20] have proposed possible solutions to improve a series-connected two-battery module. The protection of energy storage in electric wheelchair batteries guarantees the safety of its users.

2. System Specification

We developed a block diagram of the battery-balancing system and battery-protection circuit, as shown in Fig. 1. Through a voltage-detection circuit, current-detection circuit, and battery-balance controller, the battery-balancing system can passively balance the voltage of two batteries by extracting voltage from the higher-potential battery to the lower-potential battery.

* Corresponding author. E-mail address: bob84425@gmail.com

A digital signal processor (DSP) was used to measure, monitor, and convert the received battery voltage through an internal analog-to-digital converter and transmit the signal to the double-active switch of the buck-boost circuit. The PWM signal was modulated to control the on and off states of the switch to balance the current and voltage.

The battery protection circuit was composed of a temperature-detection circuit, current-detection circuit, and battery-protection control circuit. During the charging or discharging stage of the series-connected two-battery module, the battery-protection circuit detected and transmitted voltage signals collected from the parameters of the surrounding environment, such as the charging current, discharging current, and temperature, to the DSP. These voltage signals were then converted through the internal analog-to-digital converter and transmitted to the corresponding switches for modulation and control.

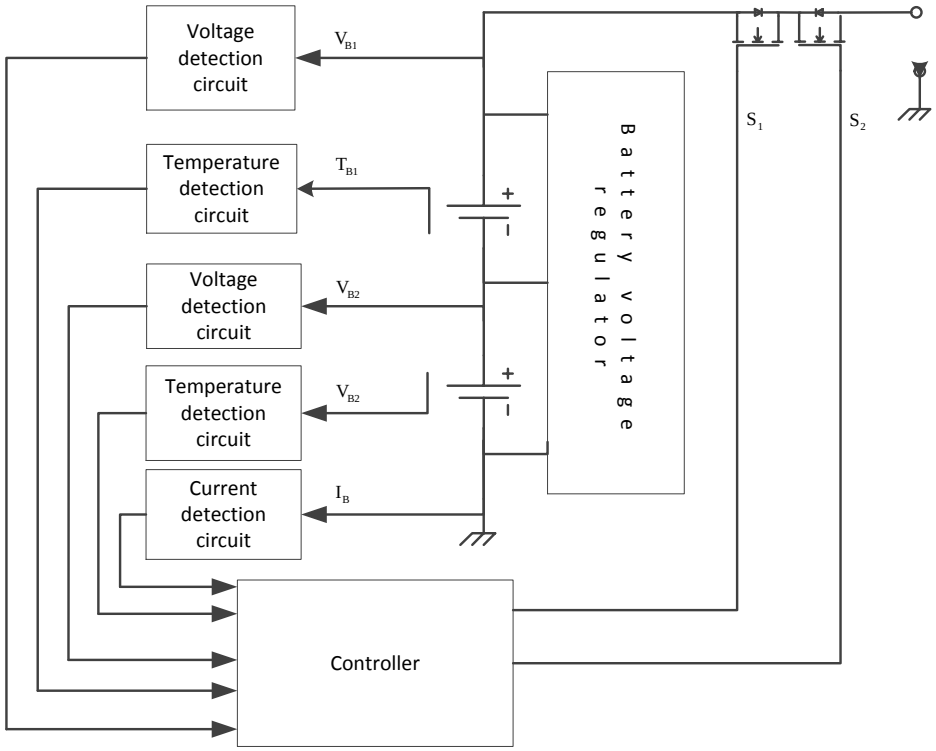

Fig. 1 BMS block diagram

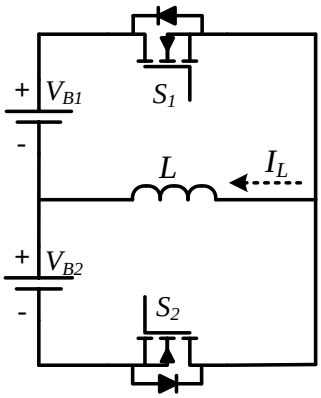

Fig. 2 Bidirectional buck-boost circuit diagram

In this paper, we focused on the development of the DSP to understand the operating state of the battery based on the digital signals and to trigger the protection and balancing actions when necessary.

Using a bidirectional buck-boost circuit, the battery voltage in serially connected batteries can be regulated, as shown in Fig. 2.

The bidirectional buck-boost circuit was composed of two power transistors S1, S2 and an inductor L to form a synchronous rectified, bidirectional power-transfer buck-boost circuit. Thus, the battery voltage can be regulated by transferring power from the higher-voltage battery to the lower-voltage battery. Starting with battery B1 as the basis, the operation was divided into two modes: buck mode and boost mode. Buck mode lowered the voltage of battery B1, whereas boost mode increased the voltage of battery B1.

When the battery voltage V_{B1} was higher than V_{B2}, the upper switch S_1 was turned on while the lower switch S_2 was turned off, forming a discharge path from battery B_1 to inductor L, as shown in Fig. 3(a). This discharge current flowed through and stored power in inductor L. Next, the upper switch $S1$ was turned off while the lower switch $S2$ was turned on, forming a charging path from inductor L to battery B_2, as shown in Fig. 3(b). This inductor current I_L flowed into battery B_2, charging the battery. In this operating mode, battery B_1 was discharged while battery $B2$ was charged, effectively reducing the voltage of B_1 and increasing the voltage of B_2.

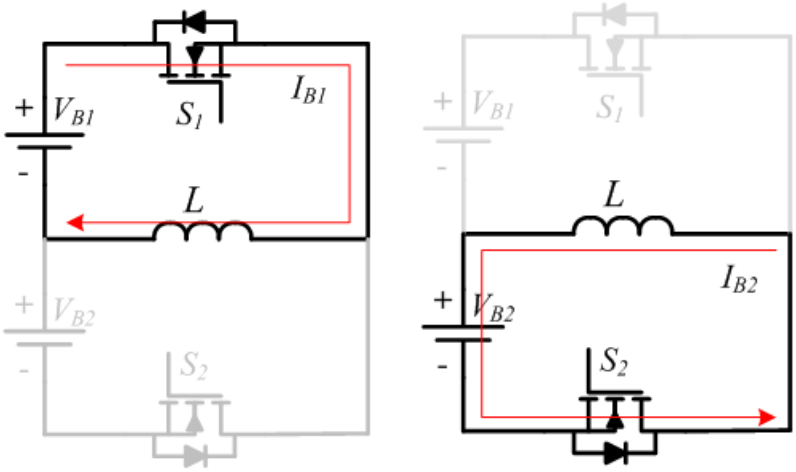

(a) S_1 on, S_2 off (b) S_1 off, S_2 on

Fig. 3 Buck mode circuit diagram (a) (b)

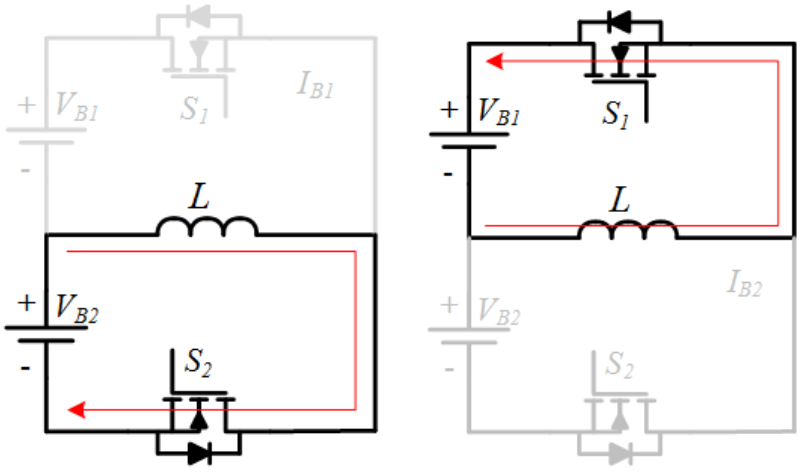

(a) S_2 on, S_1 off (b) S_2 off, S_1 on

Fig. 4 Boost mode circuit diagram (a) (b)

On the other hand, when the battery voltage V_{B1} was lower than V_{B2}, the lower switch S_2 was turned on while the upper switch S_1 was turned off, forming a discharge path from battery B_2 to inductor L, as shown in Fig. 4(a). This discharge current flowed through and stored power in inductor L. Next, the lower switch S_2 was turned off while the upper switch S_1 was turned on, forming a charging path from inductor L to battery B_1, as shown in Fig. 4(b). This inductor current I_L flowed into battery B_1, charging the battery. In this operating mode, battery B_1 was charged while battery B_2 was discharged, effectively increasing the battery voltage of B_1 and reducing the battery voltage of B_2.

3. Simulation Results

The circuit operation timing simulation in buck mode is shown in Fig. 5, where V_{gs1} and V_{gs2} were the operating gate voltages of switch S_1 and S_2 respectively, I_{B1} was the discharging current of battery B_1, and I_{B2} was the charging current of battery B_2.

Similarly, the circuit operating timing simulation in boost mode is shown in Fig. 6, where V_{gs1} and V_{gs2} were the operating gate voltage of switch S_1 and S_2 respectively, I_{B1} was the charging current of battery B_1, and I_{B2} was the discharging current of battery B_2.

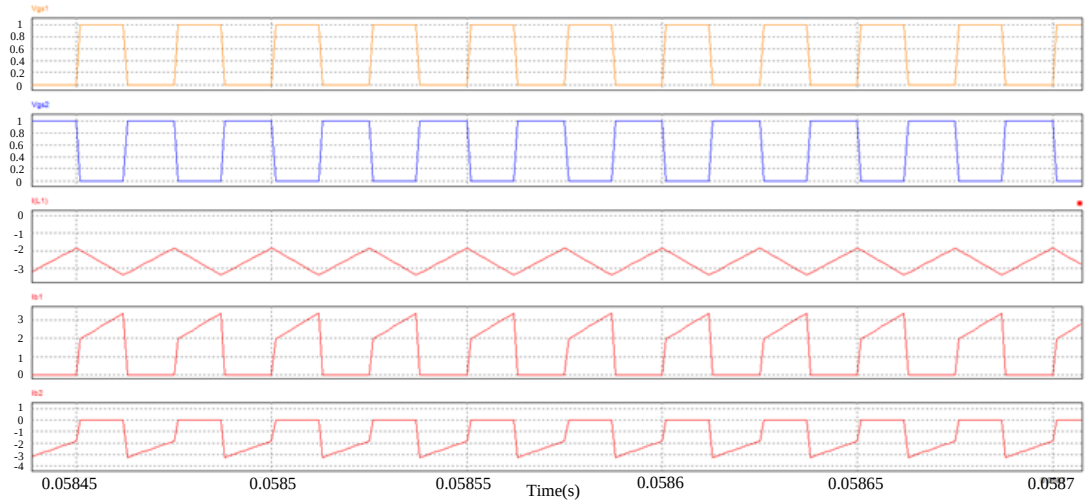

Fig. 5 Buck-mode timing simulation of a buck-boost circuit

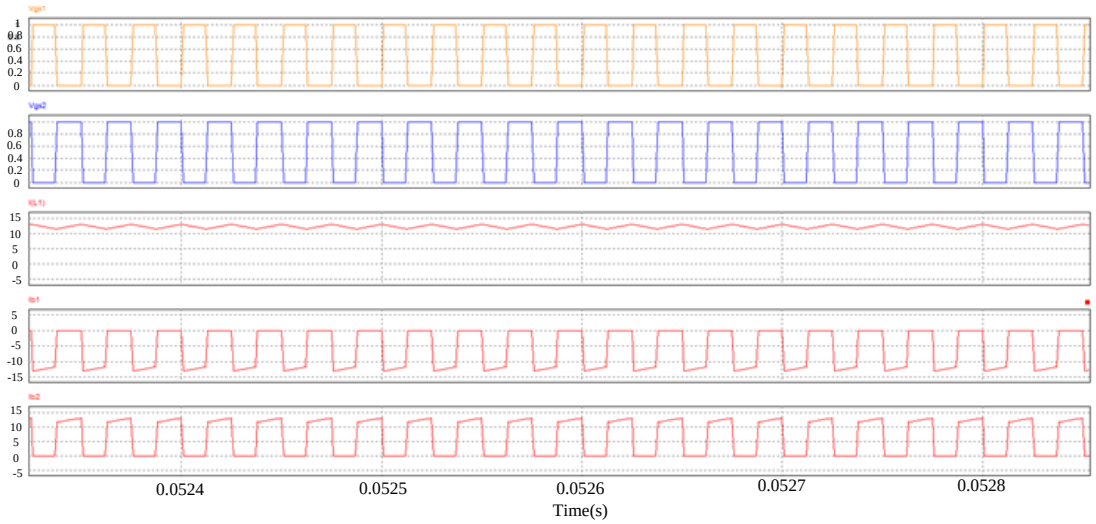

Fig. 6 Boost-mode timing simulation of a buck-boost circuit

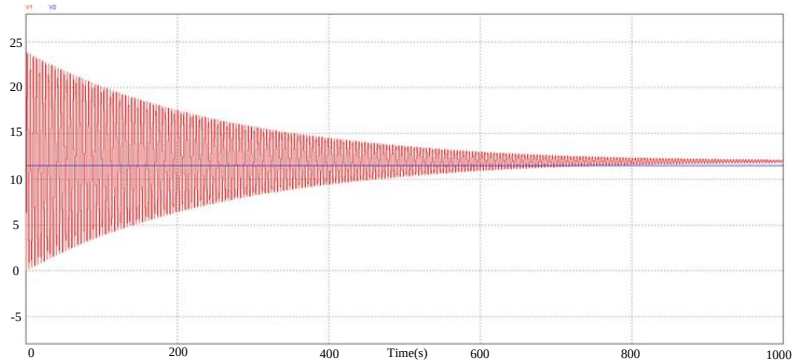

Fig. 7 Simulation result of the battery-balancing operation

Fig. 7 shows the simulation result of battery-balancing operations. The B_1 and B_2 voltages were 12.7 V and 12.08 V, respectively, with a 0.72-V delta. The battery voltage difference was clearly reduced to within 0.1 V during the measurement timeframe.

Fig. 8 shows the simulation result of the battery's voltage protection. When the battery voltage was higher than 30 V, the charging switch was turned on to stop the external voltage from charging the battery. As the battery voltage recovered to 24 V, the protection was switched off to allow normal operation in a closed circuit. When the battery voltage was lower than 21 V, the discharging switch was turned on to stop the battery from discharging to the load. Again, as the battery voltage recovered to 24 V, the protection was switched off to allow normal operation in a closed circuit.

Fig. 9 shows the simulation result of the battery's temperature protection. When the temperature voltage was higher than 4.43 V (lower than -1 ℃) or lower than 2.5 V (higher than 43 ℃), the charging and discharging switch were turned on to form an open circuit, activating the battery's temperature-protection mechanism. If the temperature was within the operational range, both switches were turned off for normal operation in a closed circuit.

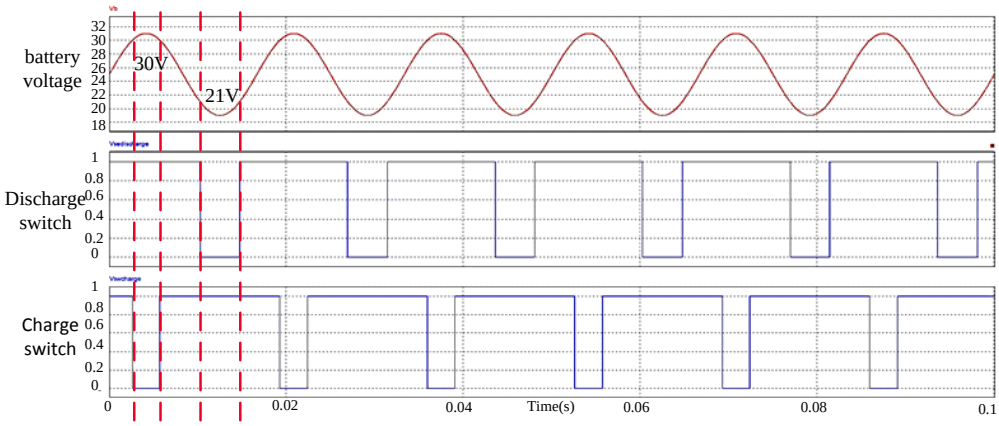

Fig. 8 Simulation result of the battery's voltage protection

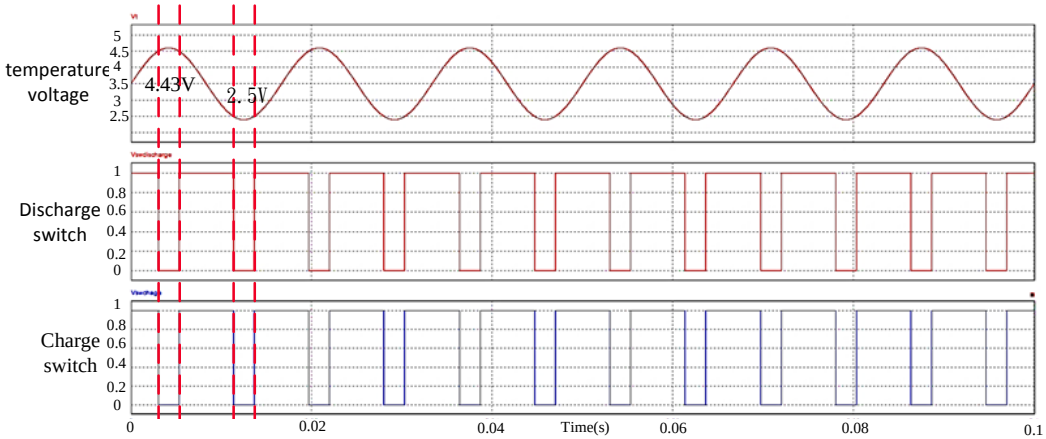

Fig. 9 Simulation result of the battery's temperature protection

4. Conclusion

This paper successfully developed a BMS with a voltage-balancing and -protection mechanism, to achieve a voltage-balancing modulation, voltage monitor, current monitor, and temperature monitor for the battery. The description of these applications is as follows:

Battery voltage balancing modulation: Monitor and modulate the charging and discharging current of each battery in serially connected batteries. Effectively increase battery's lifespan via voltage regulation by balancing the batteries to within a 0.1-V range.

Battery voltage monitor: When the battery voltage was higher than 30 V, the charging switch was turned on to form an open circuit to protect the battery from over-voltage charging. When the battery voltage was lower than 21 V, the discharging switch was turned on to form an open circuit to protect the battery from over-voltage discharging.

Battery current monitor: When the battery current was higher than 25 A for longer than 1 s, the charging switch was turned on to form an open circuit to protect the battery from over-current charging. When the battery current was higher than 60 A for longer than 1 s, the discharging switch was turned on to form an open circuit to protect the battery from over-current discharging.

Battery temperature monitor: When the battery temperature was higher than 43 ℃ or lower than -1 ℃, the charging and discharging switches were turned on to form an open circuit, protecting the battery from operating outside its safe operating region.

5. Outlook

The voltage-balancing and battery-protection mechanisms for a battery were developed successfully in this study. However, the safety parameters, electromagnetic compatibility (EMC), and tolerance need to be improved for practical applications. The description of these aspects is as follows:

Safety parameters include settings for over-voltage, over-current, and over-temperature operations. If the parameters were too loose, batteries would be damaged before the protection mechanism was activated. On the other hand, if the parameters were too tight, the protection mechanism would activate within the safe operating region, interrupting the normal operation of electric wheelchairs. Thus, the definition of the safety parameters is critical.

Electromagnetic interference (EMI) refers to the interference of the designed battery-balancing circuit and the battery-protection circuit with other electronic systems. Design in accordance with available EMI and EMC standards for power converters is suggested.

Finally, tolerance refers to the operation of the designed battery-balancing circuit and the battery-protection circuit outside its safe operating region. Design in accordance with UL or CE standards for power converters is suggested.

References

[1] M. Wada and F. Kameda, “A joystick car drive system with seating in a wheelchair,” 2009 35th Annual Conference of IEEE Industrial Electronics, IEEE Press, November 2009, pp. 2163-2168.
[2] Y. K. Kim, Y. H. Cho, N. C. Park, S. H. Kim, and H. S. Mok, “In-Wheel motor drive system using 2-phase PMSM,” 2009 IEEE 6th International Power Electronics and Motion Control Conference, Wuhan, May 2009, pp. 1875-1879.
[3] P. Kishore, M. Ananth, S. Chidambaram, B. Vivekanandan, and N. A. Gounden, “Solar Based Hybrid Electric Powered Wheelchair,” 2013 Texas Instruments India Educators' Conference, IEEE Press, April 2013, pp. 18-24.
[4] M. Wada, “Holonomic and omnidirectional wheelchairs with synchronized 4WD mechanism,” 2007 IEEE/RSJ International Conference on Intelligent Robots and Systems, IEEE Press, November 2007, pp. 1196-1202.
[5] R. H. Putra, A. G. W. Rahman, E. S. Ningrum, and D. S. Purnomo, “Design and stress analysis on electric standing wheelchair,” 2017 International Electronics Symposium on Engineering Technology and Applications (IES-ETA), IEEE Press, September 2017, pp. 112-117.
[6] K. Vitols and A. Podgornovs, “Concept of cost-effective power-assist wheelchair's electrical subsystem,” 2017 5th IEEE Workshop on Advances in Information, Electronic and Electrical Engineering (AIEEE), IEEE Press, November 2017, pp. 1-4.
[7] K. K. Ayten, A. Dumlu, and A. Kaleli, “Real-time trajectory tracking control for electric-powered wheelchairs using model-based multivariable sliding mode control,” 2017 5th International Symposium on Electrical and Electronics Engineering (ISEEE), IEEE Press, October 2017, pp. 1-6.
[8] M. J. Rana and M. A. Abido, “Energy management in DC microgrid with energy storage and model predictive controlled AC–DC converter,” IET Generation, Transmission & Distribution, vol. 11, no. 15, pp. 3694-3702, November 2017.

[9] Q. Xu *et al*., "A Decentralized Dynamic Power Sharing Strategy for Hybrid Energy Storage System in Autonomous DC Microgrid," in IEEE Transactions on Industrial Electronics, vol. 64, no. 7, pp. 5930-5941, July 2017.

[10] D. Kumar, F. Zare, and A. Ghosh, "DC Microgrid Technology: System Architectures, AC Grid Interfaces, Grounding Schemes, Power Quality, Communication Networks, Applications, and Standardizations Aspects," in IEEE Access, vol. 5, pp. 12230-12256, June 2017.

[11] A. Merabet, K. Tawfique Ahmed, H. Ibrahim, R. Beguenane, and A. M. Y. M. Ghias, "Energy Management and Control System for Laboratory Scale Microgrid Based Wind-PV-Battery," IEEE Transactions on Sustainable Energy, vol. 8, no. 1, pp. 145-154, Jan. 2017.

[12] M. Farrokhabadi, S. König, C. A. Cañizares, K. Bhattacharya, and T. Leibfried, "Battery Energy Storage System Models for Microgrid Stability Analysis and Dynamic Simulation," IEEE Transactions on Power Systems, vol. 33, no. 2, pp. 2301-2312, March 2018.

[13] S. Sharma, S. Bhattacharjee, and A. Bhattacharya, "Grey wolf optimisation for optimal sizing of battery energy storage device to minimise operation cost of microgrid," IET Generation, Transmission & Distribution, vol. 10, no. 3, pp. 625-637, March 2016.

[14] B. Xie, Y. Liu, Y. Ji, and J. Wang, "Two-stage battery energy storage system (BESS) in AC microgrids with balanced state-of-charge and guaranteed small-signal stability," Energies, vol. 11, no. 2, pp. 1-14, February 2018.

[15] B. V. Mbuwir, F. Ruelens, F. Spiessens, and G. Deconinck, "Battery energy management in a microgrid using batch reinforcement learning," Energies, vol. 10, no. 11, pp. 1846-1-1846-19, November 2017.

[16] A. Hussain, V. H. Bui, and H. M. Kim, "Impact analysis of demand response intensity and energy storage size on operation of networked microgrids," Energies, vol. 10, no. 7, pp. 882-1 - 882-19, June 2017.

[17] A. Hussain, V. H. Bui, and H. M. Kim, "Fuzzy logic-based operation of battery energy storage systems (BESSs) for enhancing the resiliency of hybrid microgrids," Energies, vol. 10, no. 3, pp. 271-1 - 271-19, February 2017.

[18] A. Hussain, V. H. Bui, and H. M. Kim, "An energy-based control strategy for battery energy storage systems: a case study on microgrid applications," Energies, vol. 10, no. 5, pp. 215-1-215-20, February 2017.

[19] S. Y. Yu, H. J. Kim, J. H. Kim, and B. M. Han, "SoC-based output voltage control for BESS with a lithium-ion battery in a stand-alone DC microgrid," Energies, vol. 9, no. 11, pp. 924-1 - 924-15, November 2016.

[20] Y. S. Kim, C. S. Hwang, E. S. Kim, and C. Cho, "State of charged-based active power sharing method in a stad alone microgrid with high penetration level of renewable energy sources," Energies, vol. 9, no. 7, pp. 480-1 - 480-13, June 2016.